

DAA/LANGLEY  
NAG-1-654

IN-34

Enhanced Viscous Flow Drag Reduction  
Using Acoustic Excitation

64858

P.21

Semi-Annual Progress Report for the  
Period Ending September 14, 1986

Dr. Robert T. Nagel  
Principal Investigator  
Mechanical and Aerospace Engineering  
Box 7910  
North Carolina State University  
Raleigh, North Carolina 27695-7910

Grant Number NAG-1-654

(NASA-CR-180692) ENHANCED VISCOUS FLOW DRAG  
REDUCTION USING ACOUSTIC EXCITATION  
Semiannual Progress Report, period ending 14  
Sep. 1986 (North Carolina State Univ.) 21  
F Avail: NTIS HC A02/MF A01 CSCL 20D G3/34

N87-27127

Unclas  
0064858

NASA Technical Officer: John B. Ander

## 1. Introduction

It is known that proper manipulation of a turbulent boundary layer with a thin stationary plate spanning the flow can cause a reduction in the skin friction drag downstream of the manipulation point. These devices have several names such as "BLADES", (boundary layer alteration devices) or "LEBU's", (large eddy break-up devices). Use of this type of device was developed by Yajnik and Acharya (1977); Corke, Guezennec & Nagib (1979); Hefner, Weinstein & Bushnell (1979), and others. Work by these investigators has produced a marked evolution in the performance and understanding of certain configurations.

This technology is, however, not well developed. This is clear when one looks at the repeatability of the various experiments by Hefner, Anders and Bushnell (1983). Anders (1985) has pointed out that changes in the microgeometry of the device may cause significant changes in the results. Mildly stroking the LEBU blade with fine sandpaper can significantly alter the data but reductions in drag consistently occur.

Several mechanisms have been suggested by Corke, Nagib and Guezennec (1982) by which manipulator plates are able to remove the large eddy structure from the boundary layer and reduce the skin friction drag. These suggested mechanisms include attenuation of the normal velocity component of the large scale structure by the manipulators and the redistribution of the turbulent kinetic energy by the blade wake.

Another possible scenario based upon the work of Liss and Usol'tsev (1973), assumes that the manipulator blade acts as an airfoil in a gusty environment. As large eddies in the boundary

layer impinge on the manipulator blade, the blade experiences a small fluctuation in the effective angle of attack. The resulting change in circulation would produce vortex shedding at the manipulator trailing edge. This vortex could then partially cancel the vorticity associated with the incident turbulent eddy. With a reduction in the large eddy content, the momentum transfer from the mean flow to the wall would be reduced leading to a reduction in the momentum thickness and associated wall drag. If this proposed mechanism is correct it would be possible to influence the process by directing an acoustic wave toward the LEBU. If the acoustic pulse is phase locked to the incident flow, the canceling vortex shed from the manipulator plate could be modified by the acoustic pressure to enhance the large eddy cancellation process.

In a recent paper by Papathanasiou & Nagel (1986) a new phenomenon associated with drag reduction using blades was reported. That paper gives evidence that the proper acoustic signal directed from the wind tunnel floor to the LEBU trailing edge can indeed be used to enhance the drag reduction obtained with the boundary layer alteration device. The acoustic signal is generated from a hot-film probe positioned upstream of the LEBU in line with the location of the acoustic input. The acoustic signal occurs in response to only large eddies in the turbulent boundary layer. The signal is time delayed by an amount equal to the eddy convection time between the hot-film probe and the LEBU trailing edge. The additional acoustic pulse applied to the LEBU blade apparently modifies the vortex shedding

from the blade and increases the large eddy cancellation. This work is described in the final report for NASA grant NAG-1-424, (Nagel, 1986) and in a paper by Papathanasiou & Nagel (1986).

The goal of this work is to verify the behavior of the flow when subjected to this phase locked acoustic excitation and to optimize the important parameters in the excitation process. Results indicate that optimization of the process is possible and that drag reduction can persist downstream and slowly spread in the spanwise direction.

## 2. Experimental Apparatus & Basic Phenomenon

The experiment is housed in the NCSU Low Speed Boundary Layer Wind Tunnel described by Nagel & Alaverdi (1985). The test section is nominally 1.0m x 0.4m x 7.0m long with an adjustable ceiling set for zero pressure gradient flow. A schematic of the test section is shown in figure 1. The boundary layer scoop at the beginning of the test section,  $x = 0.0m$ , completely removes the boundary layer which forms on the contraction floor. The test section boundary layer then starts at  $x = 0.0m$  and grows in a manner which agrees with standard predictions such as those available in the text by Cebecci and Bradshaw (1977). A sand paper boundary layer trip is installed across the span of the test section between  $x = 4cm$  and  $x = 25cm$ . The trip establishes a fully developed turbulent boundary layer at the LEBU with a complete range of length scales. With the trip installed, the resulting turbulent boundary layer also grows in accordance with standard turbulent boundary layer predictions as shown by Papathanasiou & Nagel (1986).

The large eddy break-up device consists of a single blade, with a chord equal to nine tenths of the local boundary layer thickness (3.6 cm). The device was carefully fabricated from stainless steel shimstock 0.0203cm (0.008 inches) thick and mounted across the span of the test section at 2.0m from the test surface leading edge. The blade extends through the walls of the test section at a height above the wind tunnel floor equal to 80 percent of the local boundary layer thickness. The boundary layer thickness,  $\delta$ , is determined as the location where  $u/U_e = 0.995$ . The device was secured outside the wind tunnel on an independent stand that allows adjustment of the blade height, angle of attack and blade tension. Independent adjustment of both ends of the blade is possible. This is the same basic configuration described in the final report for grant NAG-1-424, (Nagel, 1986).

The experimental arrangement to acoustically excite the manipulator blade utilizes a hot-film probe mounted  $2.5\delta$  upstream of the blade trailing edge at a height above the test surface approximately equal to the height of the blade. This is the same location used in the earlier work.

The signal from the eddy detector probe is processed in such a way so only that part of the signal corresponding to large eddies causes an input to the acoustic driver. The resulting acoustic input to the blade is a signal with approximate character and duration equal to the anemometer's response to the large incident eddies.

Basic evidence of the drag reduction due to the acoustic excitation is shown in figure 2 where the momentum thicknesses for the plain test surface are compared to those obtained with

the blade only and with the acoustically excited blade. The eddy detector probe was installed for all three cases, but was not active for measurements obtained for the plain case or the case using the blade without acoustic excitation. The data were obtained along the test surface centerline downstream of the point of acoustic excitation. The momentum thickness at any point  $x$  represents all the momentum loss between the test surface leading edge and the particular measurement point. Since the pressure gradient is zero, the slopes of the curves in figure 2 represent the skin friction coefficient along the surface. The reduced slope and skin friction coefficient that occur for the blade with and without acoustic excitation is clear. Furthermore, since the value of momentum thickness for the acoustically excited blade falls below that of the plain case when  $x$  is greater than 3.6m, one may conclude net drag reduction occurs for this region. One should also note that data for the plain configuration (without the LEBU) are unaffected when acoustic excitation is applied to the flow and the blade is removed. The results of Figure 2 may serve as an example of typical results with which to compare the results of optimization.

### 3. Optimization of Process

When acoustic excitation is applied to the large eddy break-up blade, there is a reduction in the peak cross-correlation function measured between the upstream eddy detector probe and a second hot-film probe positioned downstream of the blade at the same height above the test surface. As expected the cross-correlation coefficient goes to zero as the downstream probe location

is moved more than  $10 \delta$  downstream. One should note that the upstream probe is the fixed eddy detector probe located  $2.5 \delta$  upstream of the LEBU trailing edge. Within one or two boundary layer thicknesses downstream of the blade trailing edge the peak cross-correlation coefficient (CCF) is reduced from about 20% to near zero by the addition of the proper phased locked acoustic signal. This single measurement of the reduction in the coherent large eddy structure provides a quick method to optimize the acoustic signal. If one defines  $R_c$  as the ratio of the peak CCF with acoustic excitation to the peak CCF without excitation, then one can assume that the large eddies impinging on the blade are more effectively canceled when  $R_c$  is less than 1.0 and a minimum.

The three optimized parameters include the reference voltage, the time delay and the amplitude of the acoustic input. These three quantities are illustrated in figure 3. The reference voltage level determines which excursions of the anemometer response are recognized as large eddies. Since the eddy detector probe is positioned near the intermittent region of the boundary layer, large reductions in the velocity are assumed to correspond to large eddy passing. The reference voltage thus sets a threshold which triggers the processor response resulting in an acoustic input to the blade. The delay time between eddy detection and the processor output, and the amplitude of the resulting acoustic signal are both adjustable with the processor.

Figure 4 shows the existence of a distinct minimum in  $R_c$  as the reference voltage,  $V_r$ , is varied. Low values of  $V_r$  trigger

the acoustic input for only the largest eddies, whereas high values of  $V_r$  cause an acoustic response for most of the anemometer signal. These data were obtained with a time delay of approximately 10 milliseconds corresponding to the approximate eddy convection time between the eddy detector probe and the LEBU trailing edge. The acoustic amplitude used was 101 dB. For reference voltages significantly above the optimum value, the acoustic input increases the peak cross-correlation function. When  $V_r$  is below the optimum, the peak CCF is still slightly reduced. The eddy cancellation process thus seems most effective when adjusted to respond to only the large scale turbulence. Acoustic input in response to a more complete range of eddy length scales may be improperly coupled to the blade because the blade chord is of the order of the length scale associated with the large eddies.

The turbulence intensity measured from the eddy detector probe was approximately 2%. This detector probe is in the outer boundary layer in a region of high intermittancy. Figure 4 shows the reference voltage normalized by the DC voltage,  $V_o$ , from the eddy detector probe. Thus,  $(1-V_r/V_o)$  is approximately the proportion of turbulent fluctuations that trigger acoustic pulses. The optimum performance of the excitation occurred when  $(1-V_r/V_o)$  was set approximately 1/2% larger than the turbulence intensity. For the case shown in figure 4, triggering on only the largest 2.7% of the velocity excursions produced the optimum results.

As the reference voltage is varied from low values to higher values the average frequency of acoustic input pulses also



increases. The average pulse frequency is easily determined by counting the pulses over a long time interval. Figure 4 also shows the average number of acoustic pulses from the processor as a function of reference voltage. Corrsin and Kistler (1955) suggest that the large eddy passing frequency may be approximately predicted by  $U_e/(2.5 \delta)$ . For the test case examined here, this frequency corresponds to approximately 110 Hz. It is encouraging to note that the optimum value of the reference voltage occurs when the processor responds at the approximate large eddy passing frequency. Data obtained from other configurations are consistent with these results.

The time delay for the processor was also optimized. Figure 5 shows the minimum peak cross-correlation ratio occurs at a delay time corresponding to approximately 9.5 msec. This is the large eddy convection time between the eddy detector probe and the blade trailing edge as suggested by Kovasznay, Kibens and Blackwelder (1970). These results also support the notion of modified large eddy cancellation by the acoustic excitation. The reference voltage for these data was near optimum and the RMS acoustic level for sound between 0 and 2000 Hz. remained at approximately 101 dB.

The sound pressure level of the acoustic input at the LEBU trailing edge is not easily measured. Difficulties occur because of the existence of the mean flow, the wake of the LEBU and the turbulence in the boundary layer. The acoustic amplitude can, however, be measured outside the test section in a zero flow environment. The data of figure 6 have therefore been gathered

by measuring the cross-correlation functions in the normal manner with various excitation amplitudes. For the same power settings, the OASPL at the blade height above the orifice was then measured outside the tunnel. The test section floor was modeled with a square flat surface (0.6m x 0.6m) fabricated with the same size input port in the center. The prerecorded hot film output signal was used to trigger the pulse mechanism. In this manner the acoustic signal used to produce changes in the CCF could be reproduced. The OASPL was measured with a condenser microphone at the blade height with grazing incidence.

The sound pressure level required to influence the wake of the flat plate can be estimated. Melnik and Chow (1979) suggest a technique to predict the perturbation pressure at the trailing edge of a flat plate in an inviscid flow. For the test flow and flat plate blade used here, the predicted fluctuating pressure is 99.9 dB. This value should serve as a crude approximation for the acoustic amplitude required to influence the basic flow at the blade trailing edge.

The results of the optimization show that beneficial effects of the acoustic input are possible for a range of amplitudes. The minimum CCF occurred just before the acoustic driver entered a regime of non-linear response. At the higher values of OASPL the acoustic near field may also influence the cross-correlation between the hot-film probes. The measurements suggest an optimum acoustic amplitude exists near a sound pressure level of about 102 dB. This amplitude is 2 dB above the level predicted to influence the flow. This is a substantial increase in acoustic pressure due to the nature of the logarithmic scale for decibels.

The data shown in figures 4, 5 and 6 support the concept of enhanced eddy cancellation with an acoustic input which is phase locked to the incident large eddies. The optimum reference voltage level, (or response threshold level), the time delay and the required amplitude all support the concept of acoustic wave - large eddy interaction at the blade trailing edge. The result of this interaction is a reduction of the peak cross-correlation function across the blade and a reduction of the skin friction drag downstream as demonstrated in figure 2.

The optimization shows the most sensitive adjustment is associated with the reference voltage  $V_r$ . A deviation of only 1% in  $V_r$  from the optimum value is sufficient to significantly reduce the effectiveness of the excitation. This sensitivity in  $V_r$  may be the principle difficulty in achieving "good" drag reduction with this technique.

The distribution of momentum thickness along the wind tunnel centerline for the optimized case is compared in figure 7 with the unexcited LEBU and the plain flow cases. Near the blade the optimized excitation does not produce initial increases in momentum thickness as significant as those for the unoptimized case of figure 2. The general trend of the data is the same, but net drag reduction is achieved much earlier. The momentum thickness with optimized excitation falls below the plain flow data near  $x = 2.9$  m rather than  $x = 3.6$  m as is figure 2. Drag reduction is clearly improved and the optimization based upon the peak cross-correlation function is effective.

#### 4. Spanwise Spreading of the Phenomena

Figures 2 and 7 show enhanced drag reduction caused by acoustic excitation extends a significant distance downstream. One might expect mixing of the surrounding turbulence in the boundary layer to quickly dilute this phenomenon. Data collected across the span of the surface (cross-stream) indicate, however, that the drag reduction phenomenon spreads slowly in the transverse direction.

Limited cross-correlation data show that reductions in the cross-correlation function near the LEBU also spread spanwise as the measurements are extended downstream. Work is continuing to verify and carefully document the spreading phenomena. A second point of acoustic excitation will be installed to examine the results of two intersecting regions of enhanced drag reduction. A second signal processor has been built and is ready for use.

#### 5. Conclusions

Proper acoustic excitation of a single large-eddy break-up device can increase the resulting drag reduction and, after approximately 40 to 50  $\delta$  downstream, provide net drag reduction. Precise optimization of the input time delay, amplitude and response threshold is difficult but possible to achieve. Drag reduction is improved with optimized conditions. The possibility of optimized processing strongly suggests a mechanism which involves interaction of the acoustic waves and large eddies at the trailing edge of the large eddy break-up device. Although the mechanism for spreading of this phenomenon is unknown, it is apparent that the drag reduction effect does tend to spread spanwise as the flow convects downstream.

The phenomenon is not unique to a particular blade configuration or flow velocity, although all data have been obtained at relatively low Reynolds numbers. The general repeatability of the results for small configuration changes serves as verification of the phenomenon.

#### REFERENCES

Anders, J.B., "Large Eddy Breakup Devices as Low Reynolds Number Airfoils", SAE Paper 861769, 1986.

Cebecci, T. and Bradshaw, P., Momentum Transfer in Boundary Layer, pp. 192-197, Hemisphere Publishing Corporation, Washington, 1977.

Corke, T.C., Guezennec, Y., Nagib, H.M., "Modification in Drag of Turbulent Boundary Layers Resulting from Manipulation of Large Scale Structures", Symposium on Viscous Drag Reduction, Dallas, Texas, Nov. 7-8, 1979.

Corke, T.C., Nagib, H.M., Guezennec, Y., "A New View on Origin, Role, and Manipulation of Large Scales in Turbulent Boundary Layers", NASA CR-165861, Feb. 1982.

Corrsin and Kistler, "Free Stream Boundaries of Turbulent Flows", NACA TR 1244, 1955.

Hefner, J.N., Anders, J.B., Bushnell D.M., "Alteration of Outer Flow Structures for Turbulent Drag Reduction", AIAA paper 83-0293.

Hefner, J.N., Weinstein, L.M., and Bushnell, D.M., "Large-Eddy Break-up Scheme for Turbulent Viscous Drag Reduction", Symposium on Viscous Drag Reduction, Dallas, Texas, Nov. 7-8, 1979.

Kovaszny, L.S.G., Kibens, V., Blackwelder, R.F., "Large-Scale Motion in the Intermittent Region of a Turbulent Boundary Layer", JFM, (1970), Vol.41, pp. 283-325.

Liss, A.Y. and Usol'tsev, A.A., "Influence of Vortex-Wing Interaction on Reducing Vortex Induction", Izvestiya Vuz. Aviatsionnaya Tekhnika, Vol. 16, No. 3, pp. 5-10, 1973.

Melnik, R.E. and Chow, R., "Asymptotic Theory of Two-Dimensional Trailing Edge Flows", NASA sp-347, pp.177-249, 1979.

Mueller, T.J., "Smoke Visualization of Subsonic and Supersonic Flows (The Legacy of F.N.M. Brown)", University of Notre Dame Report UNDAS TN-3412-1, June 1978.

Nagel, R.T., "Viscous Flow Drag Reduction by Acoustic Excitation", Final Report for NASA Grant NAG-1-424, 1986.

Nagel, R.T. and Alaverdi, O. "The NCSU Low Speed Boundary Layer Wind Tunnel," 1985 SAE Transactions, vol. 6, pp 760 - 768.

Papathanasiou, A.G. and Nagel, R.T., "Boundary Layer Control by Acoustic Excitation," AIAA Paper 86-1954, 1986.

Yajnik, K.S., Acharya, M., "Non-Equilibrium Effects in a Turbulent Boundary Layer Due to the Destruction of Large Eddies", National Aeronautical Laboratory, Bangalore, NAL-BL-7, Aug. 1977.

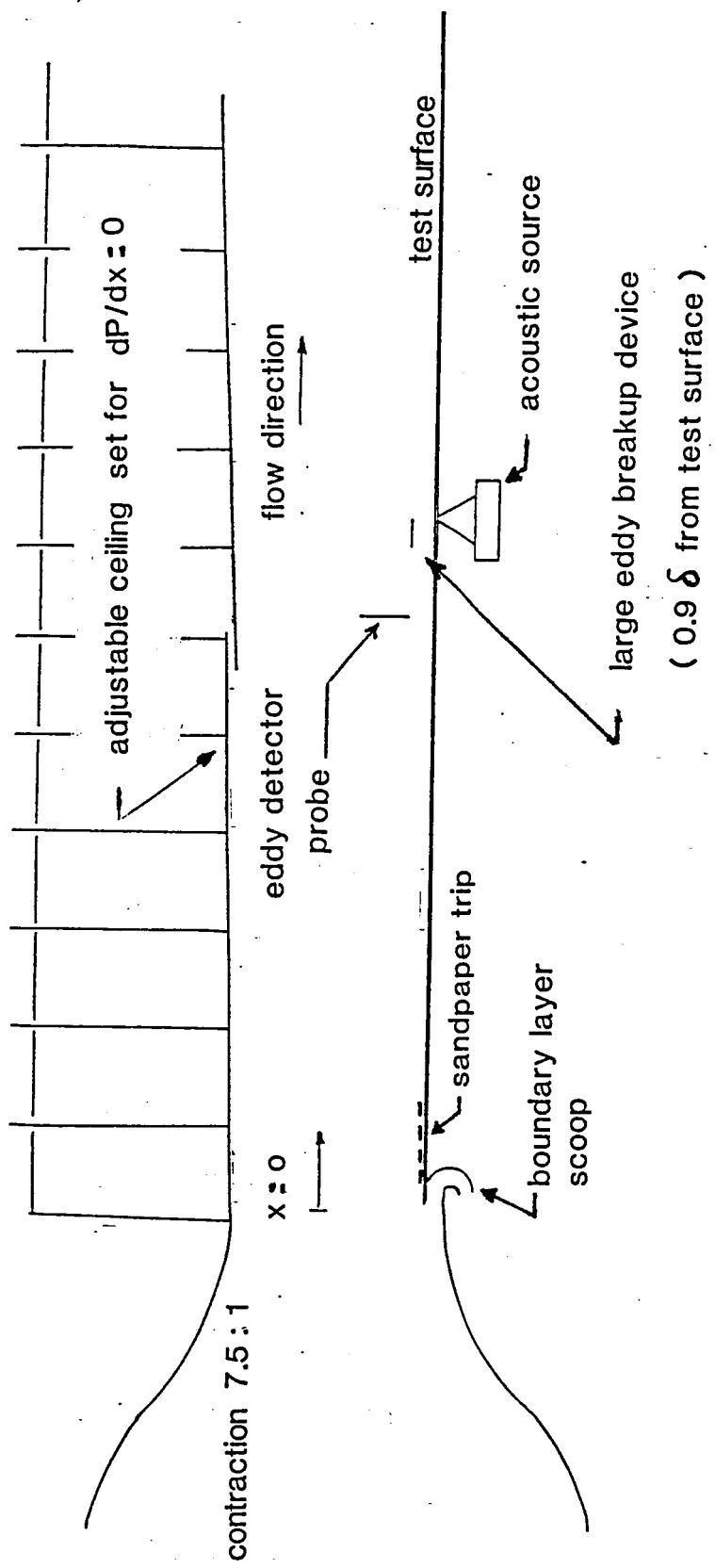


Figure 1. Wind tunnel test section.

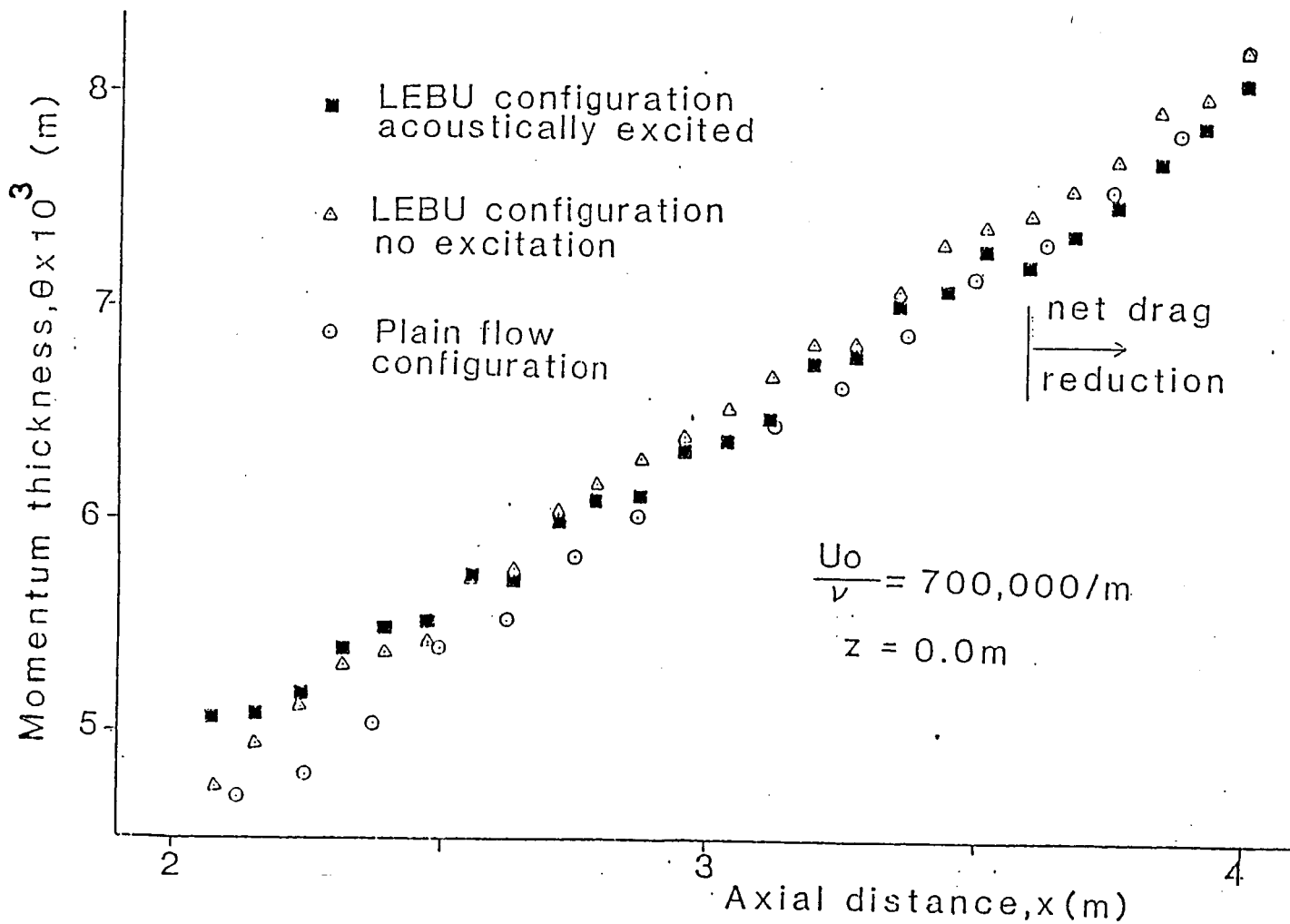


Figure 2. Momentum thickness,  $\theta$ , as a function of downstream distance,  $x$ , for various flow configurations.



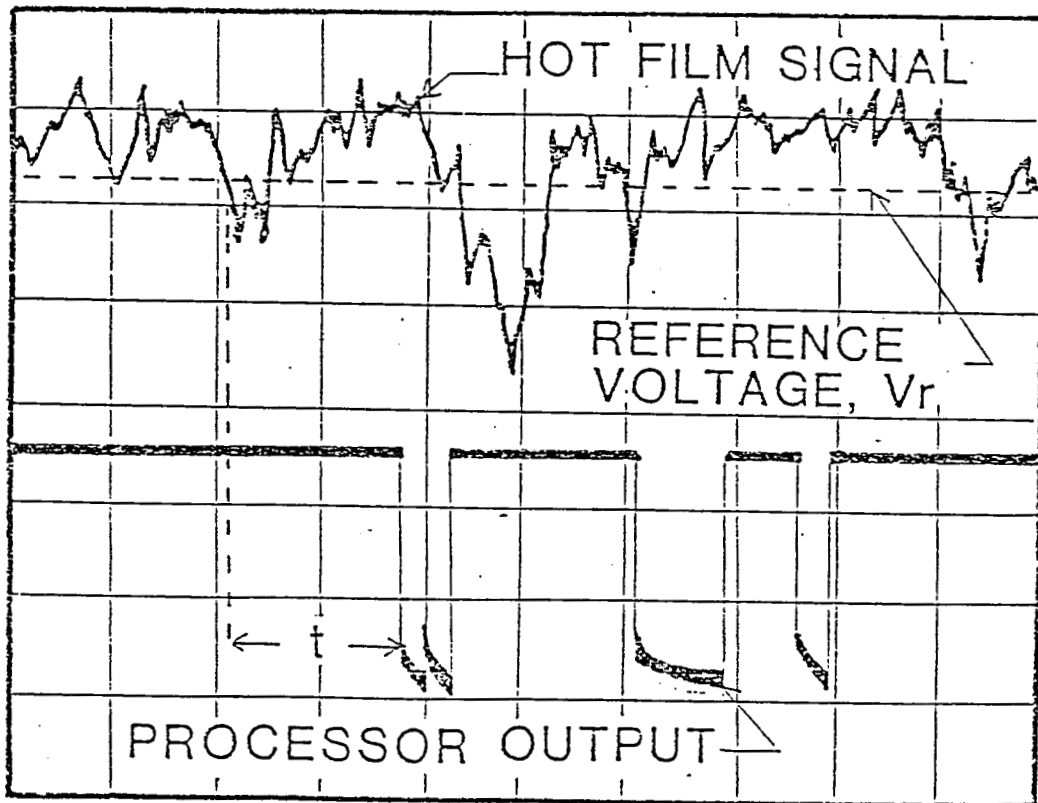


Figure 3. Processor response to the incident turbulent boundary layer.

$z=0.0$  m  
 $x=2.07$  m  
 $y=0.034$  m  
 $U_0=10.91$  m  
 $V_a=2.005$  volts  
 $CCF(L5)=0.205$

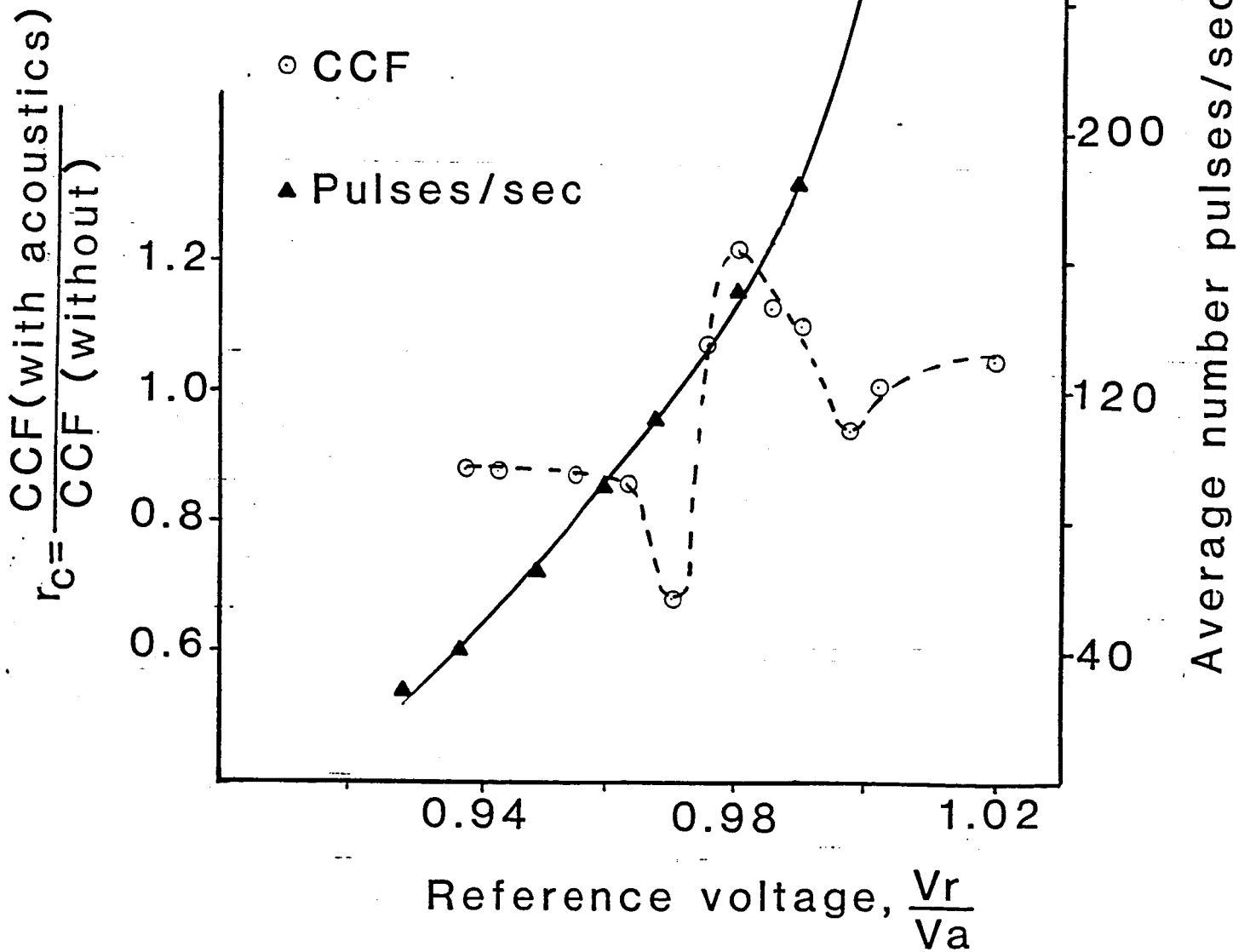


Figure 4. Normalized peak correlation,  $R_c$ , and the associated acoustic pulse frequency as a function of normalized reference voltage.

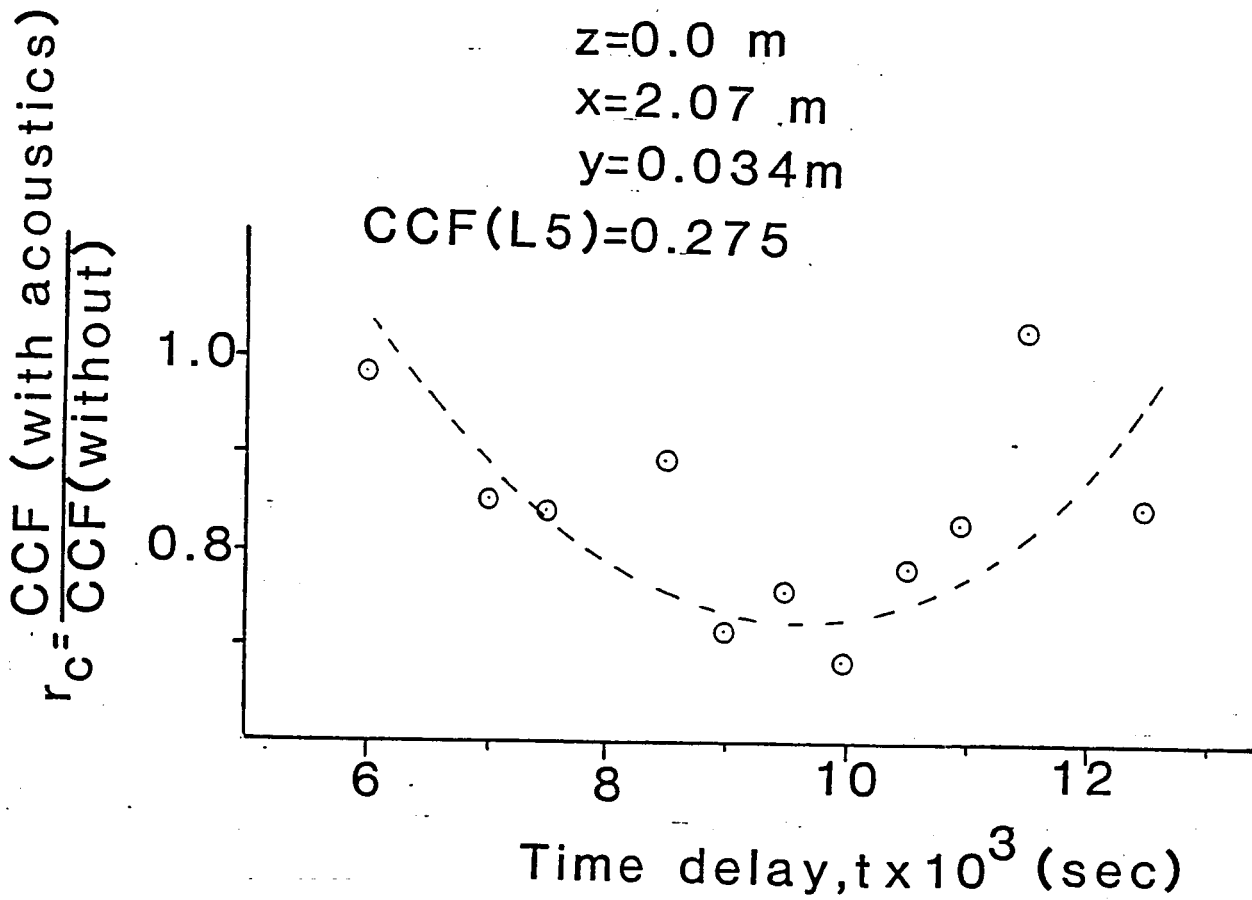


Figure 5. Variation of the normalized peak correlation,  $R_c$ , with processor time delay.

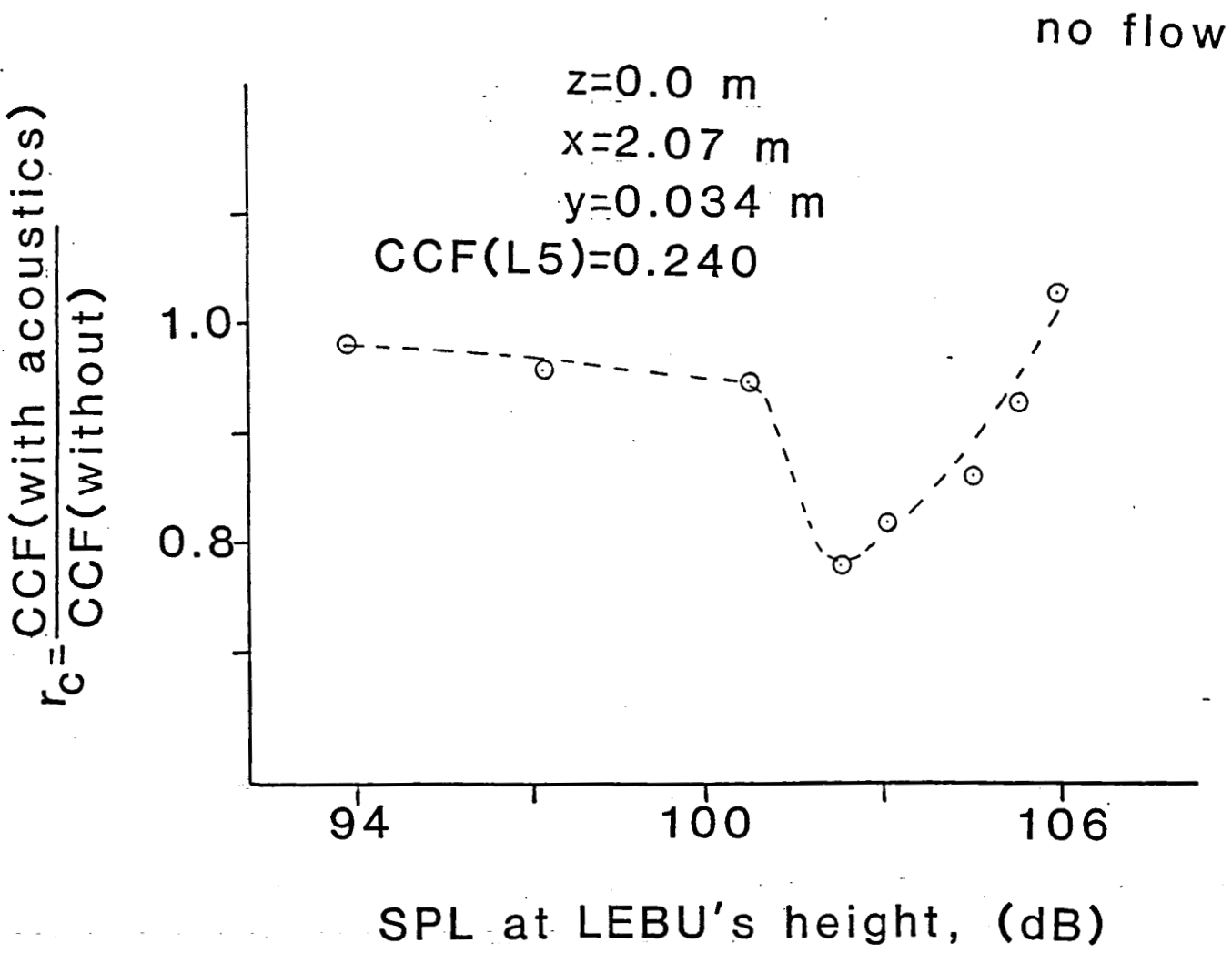


Figure 6. Variation of the normalized peak correlation,  $R_c$ , with time average SPL of acoustic excitation at the LEBU height.

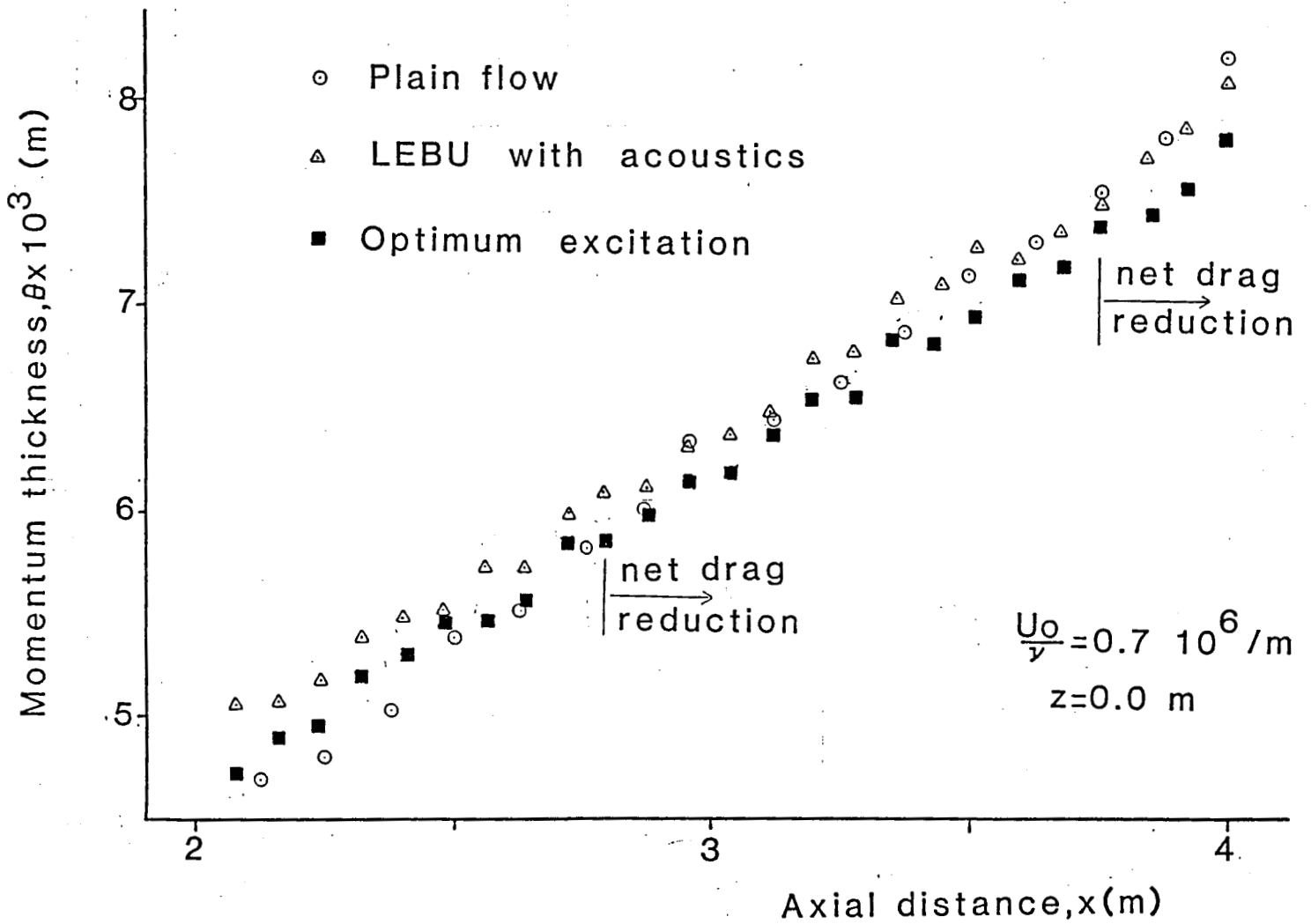


Figure 7. Momentum thickness,  $\theta$ , as a function of streamwise distance,  $x$ , for various flow configurations (with optimized acoustic excitation).